Synthesis of MOFs from Carboxylate Ligands and Its Industrial Application

Saira Mansab* and Uzaira Rafique

Department of Environmental Sciences, Fatima Jinnah Women University, The Mall, Rawalpindi 46000, Pakistan
Phone: 9251 9270050-57 Ext: 137
Fax: 9251 9271168
Corresponding Email: saira.mansab90@gmail.com;uzairaiqbal@yahoo.com

Abstract— Metal Organic Frameworks (MOFs) are widely employed as catalysts and semiconductors due to unique combination of crystalline and porous structure. The presence of polar and non-polar groups on organic linkers provides extra coordination sites for attachment of various metals. The topology of single and mixed organic ligands is tuned to higher surface area and increased porosity likely to serve as good adsorbents. The present study is based on synthesis of single and mixed ligand MOFs with Nickel as precursor. Oxalic and trimesic acid, representatives of di- and tri- carboxylates provides the organic framework. The characterization of synthesized MOFs by FTIR, XRD and SEM/EDX techniques reveal average crystallite size (0.2-3nm) and Ni is incorporated to mass percentage of 9-13%. Ni-O binding is exhibited at FTIR frequency of 493-500cm^{-1}.The application of synthesized MOFs in batch experiment at varying adsorbent dose, concentration and temperature demonstrated adsorptive capacity for dyes in the sequence Congo red (80-92%) > crystal violet (52-70%) and methyl orange (18-20%). The in-situ remediation of dyes from textile waste is also significant (71% removal) under optimum operating parameters. The study recommends the Ni-MOFs as effective adsorbents and catalysts for removal of environmental pollutants in general and azo dyes in particular.

Index Terms— Oxalic acid, Trimesic acid, Congo red, Crystal violet, Methyl orange

1 INTRODUCTION

The continuous industrial discharge and accumulation of environmental pollutants has impacted almost every aspect of life forms and physical compartments of the environment. The toxic and persistent nature of many of the pollutants poses a threat and their removal from environmental components is even more challenging [1]. To combat these problems, the researchers are continuously urging for effective and economically viable remedial measures.

Upto now various conventional methods have been adopted for removal of environmental pollutants. Of these, adsorption offers an easy, low cost and effective alternate process. Its preference is owned by the versatility and regeneration of adsorbents. However, limited numbers of structural and porous architectures available for sorption limit the usage of well established adsorbents like Activated carbon and zeolites [2]. So, research is directed at the synthesis and development of novel adsorbents with flexible artifacts.

Metal Organic Frameworks (MOFs) represent class of hybrid material that exist as infinite crystalline lattices with metal clusters and organic linkers, and possess accessible cages, tunnels and modifiable pores [3]. These properties render MOFs as efficient adsorbents for diverse applications [4]. Further, substitution of polar or non polar groups on organic backbone makes them more selective (due to enhanced hydrophilicity and hydrophobicity) for efficient removal of hazardous compounds [5]. MOFs have been successfully explored as sorbents [6]. For this purpose, various types of MOFs have been synthesized with variations in central metal, organic linkers and incorporated active species. However, limited use of MOFs [6] has been reported in the removal of dye materials. Dyes are mainly generated from textile, pharmaceutical, paper pulp and bleaching industries from where it is transferred to natural water resources and waste streams. These dyes not only change the color of the water bodies but also breakdown into toxic byproducts such as benzidine and naphthalene which are carcinogenic in nature [7].

The present research is an attempt to synthesize novel MOFs with variation of single and mixed ligand and incorporation of Ni as metal. These MOFs were further evaluated for removal of cationic, anionic dyes and pH indicator.

2 EXPERIMENTAL

Hydrothermal method [8] was adopted for synthesis with slight modification. A greener aspect was added by carrying out the synthesis under ambient temperature and pressure conditions. Further, novelty of mixed ligands (di- and tri-carbooxylate) synthesis of MOFs is also introduced. Oxalic acid and trimisic acid were used to provide organic framework for the incorporation of nickel metal. The synthesis method follows the general procedure as:

Each of the Carboxylic acid (2mmol) dissolved in absolute ethanol (12ml) was added separately, to aqueous Ni-salt solution (4mmol) under continuous stirring for 30 minutes. The solution was left undisturbed for nucleation in fume hood for 5 days.

The resultant product was filtered, washed repeatedly with ethanol, and evaporated on rotary evaporator. The dried product was pulverized and placed in desiccator till further use. In a similar fashion, mixed ligand MOFs was synthesized by adding 1:1 mixed solution of oxalic and trimesic acids to the stirring solution of metal salt.

The synthesized materials were characterized for surface and bulk properties on standardized FTIR (FTIR 8400, Shimadzu, Japan), X-rays Diffraction (Panalytical X'Pert Pro multipurpose) and SEM/EDX (JEOL JSM-6490, Japan).

The adsorptive potential of synthesized single and mixed ligand MOFs for removal of selected dyes was evaluated in batch adsorption experiment on UV-Visible spectrophotometer (UV-1601-Schimadzu, Japan) under varying conditions. Each batch was administered with three induced dye concentration of (0.01mg/L, 0.03mg/L, 0.05 mg/L) on each of the adsorbent dose (1mg, 5mg, 10mg) and working temperatures of 25°C (room temperature), 50°C, and 70°C. The absorbance of Methyl Orange, Congo Red, and Crystal Violet was recorded at 465nm, 497nm, and 590nm, respectively after full spectral scan. The adsorption (percentage removal) was calculated from the constructed standard calibration curve using the formula as.

$$\%R = \frac{Ci - Ct}{Ci} \times 100$$

3 RESULTS AND DISCUSSION

The present research provides an efficient, simple and environment friendly greener method for the successful synthesis of uni-and bi-ligand organic framework centralized around Nickel. Further, the efficacy of each of the synthesized material as adsorbent under varying experimental batch conditions is determined.

3.1 Characterization of Synthesized Materials

The synthesized products were characterized using FTIR, XRD and SEM/EDX to identify its bonding, crystallinity, morphology and elemental composition. FTIR analysis (see Figure 1) indicated the presence of organic ligand in (NiOX) at 721cm^{-1} that may be attributed to structural vibration of C-C bond [9]. The peak at 829cm^{-1} and 1300cm^{-1}-1370cm^{-1} is assigned to asymmetric stretching and symmetric vibration of υ(CO), respectively, in oxalic acid. The incorporation of metal (Nickel) into organic frame depicts sharp and intense asymmetric stretching modified to broad band at 1710cm^{-1}-1780cm^{-1}. This change might be representation of υ(OCO) due to metal binding [10].

FTIR spectrum (see Fig.1) of Ni-trimesic acid (NiT) reveals the sharp peak of C-H in-plane and out-planes bending vibration of benzene ring [11] at 1150cm^{-1}-1250cm^{-1} and 675-900cm^{-1}. On the other hand, bi-ligand Ni-MOF (NiTOX) showed C-H in plane bending in the range 1278cm^{-1}-1107cm^{-1}, whereas, C-C stretching of benzene ring is depicted at 1404cm^{-1} -1468cm^{-1}. In- plane bending vibration of υ(CO) is represented by two sharp peaks in the range 650cm^{-1} -750cm^{-1}. Ni-O coordination bond determined at 400-500cm^{-1} represents binding of metal with organic ligand [12].

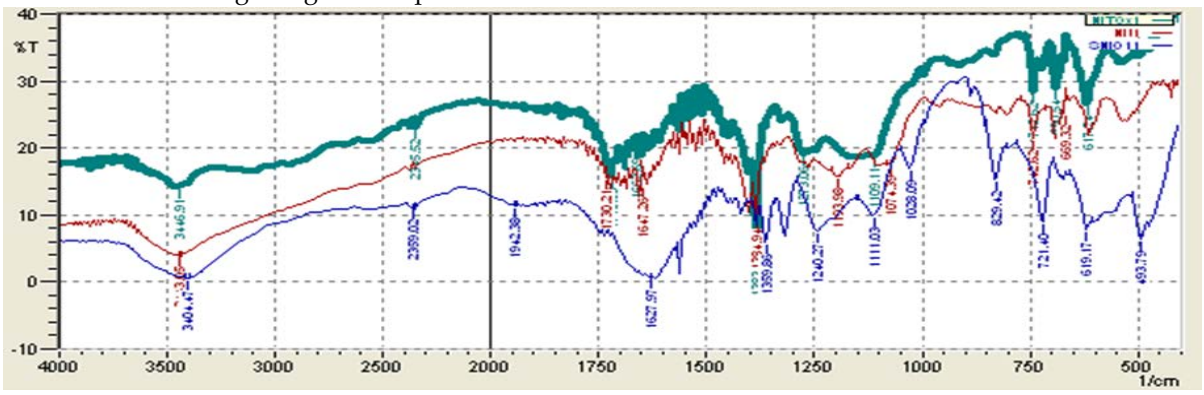

Fig. 1. FTIR Spectra of Ni based uni-and bi-ligand MOFs (a) NiOX (b) NiT (c) NiTOX

The synthesized metal-organic materials were impinged with X-rays to determine diffraction of incoming rays at definite angles by inter-spacing of layers/planes (see Fig. 2). Ni doping on oxalic acid (NiOX) shows sharp and intense peaks at 18.8°, 22.5°, 23.6°, 29.4° and 30.9° with d spacing 4.7A°, 3.9A°, 3.7A°, 3.0A° and 2.8A°, respectively. Similar pattern was observed by Rios, et al., 2012. However, emergence of small peaks diffracted at 38.9° and 47.9° may indicate unreacted NiO as impurity. On the other hand, Nickel based trimesic acid (NiT) revealed important diffractions at 19.7°, 24.3°, 27.4°, 29.5°, 32.9° and 39.0°. Furthermore, diffraction due to –COOH is observed at lower angles (18.8° and 19.7°) indicating presence of two and three groups attached to aliphatic (oxalic acid) or aromatic (trimesic acid), respectively (Yan, *et al.*, 2014). The expected metal binding through carbonyl group is demonstrated at angle of 29°-31°. However, it is interesting to note that aliphatic binding diffracts

with high intensity (close to 100) in comparison to aromatic groups.

The composite (NiTOX) synthesized by mixing equimolar ratio of aliphatic (oxalic) and aromatic (trimesic) offers unique diffraction pattern. It exhibits metal to carbonyl linkage in the range 29°-31°. It is also noted that a new peak at 33.1° of high intensity appeared as a result of aliphatic to aromatic linkage. In addition, diffracted peaks due to free –COOH aliphatic and aromatic groups diminishes in the composite. This confirms the successful synthesis of composite having both reagents. XRD pattern may conclude that the product is crystalline in nature. The crystalline nature of MOFs is reported in the literature [2].

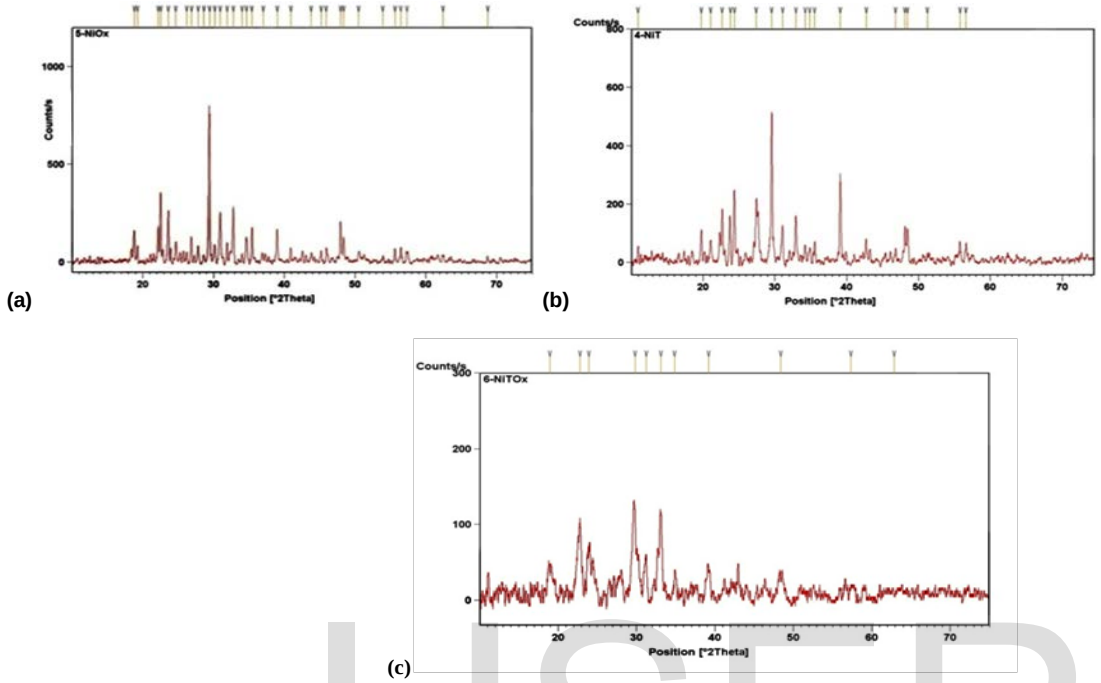

Fig. 2. XRD of synthesized Ni-based MOFs (a) NiOX (b) NiT (c) NiTOX.

Each of the synthesized Metal Organic Framework was scanned under SEM for surface morphological features and assessment of average particle size. The micrographs are reproduced in Fig. 3.

The basic organic framework of oxalic acid and trimesic acid complexed with Nickel shows beautifully arranged particles with well defined geometrical shapes. Agglomerates of cubic shapes stacked one above other defines NiOX, whereas, the same cubic geometry is more clearly attained by NiT particles. It might be attributed to the available three –COOH groups attached to aromatic ring for the later in comparison to two aliphatic in the earlier. It is suggested that higher is the number of binding groups, more regular geometrical arrangement is attained. Cubic geometry with tetrahedral arrangement for Ni-Oxalate is reported by [10]. The composite (NiTOX) exhibits agglomerates of cubes and pure cubic pattern, representing participation of both components. Further, conversion into the composite is verified by overwhelming appearance of new phase (showing interconnected cage like structure) widely seen in the image. The synthesis of such composite is the peculiar feature of the present research and not reported elsewhere.

The size determined by SEM for NiOX (1-5µm) is found slightly smaller than NiT (1.47-6µm) crystals. Whereas, composite NiTOX size is diversified over the range 24-840 nm. The study concludes that synthesized MOFs are mesoporous with definite crystalline geometry. Such characteristics features are also identified in the literature [13] for MOFs.

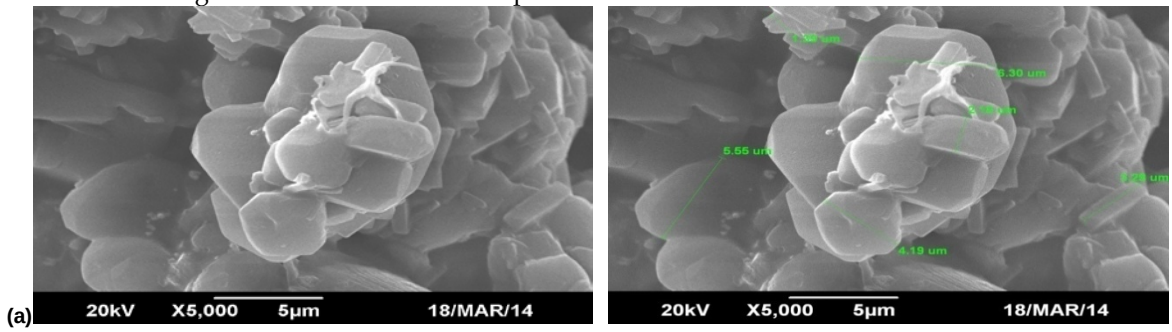

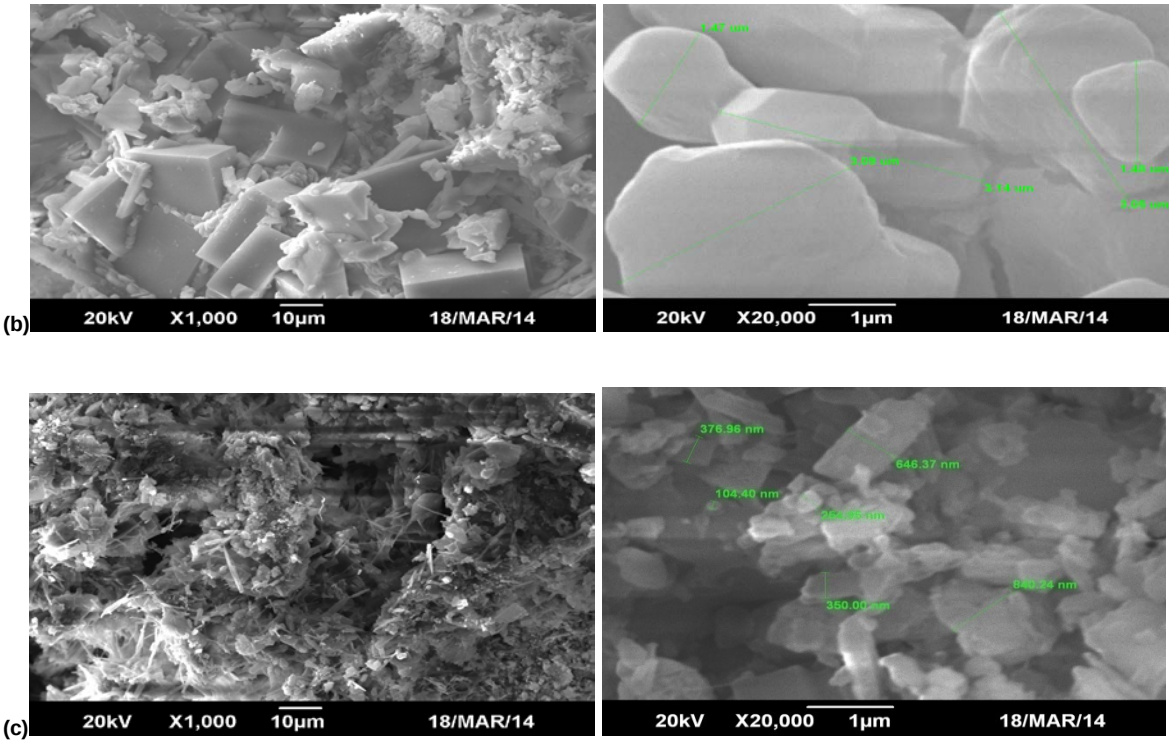

Fig. 3. SEM images of synthesized Ni-based MOFs (a) NiOX (b) NiT (c) NiTOX

The incorporation of metals into the organic framework was determined by EDX analysis. Highlights of results (given in Table 1) clearly indicates carbon and oxygen as the main constituents of each synthesized material confirming the framework (of oxalic acid and trimesic acid) is constructed mainly on these two atoms. However, variation in carbon content in NiOX and NiT can directly be related to less and more carbons in aliphatic ($C_2H_2O_4$) and aromatic ($C_9H_6O_6$), respectively. Further, carbon to oxygen ratio in the respective two MOFs (11.4:1.3) indicates more oxygen for less carbon containing compound, supported by molecular formulae. The mixed ligand composite shows carbon to oxygen ratio as 1:2, also supported by [14].

Table 1. EDX data of Ni-based uni-and bi-ligand MOFs

Sample Code	NiOX			NiT			NiTOX		
	Atom (%)	Mass (%)	Error (%)	Atom (%)	Mass (%)	Error (%)	Atom (%)	Mass (%)	Error (%)
C	7.26	4.36	6.75	41.79	30.67	3.86	31.07	22.98	3.20
O	57.85	44.99	4.65	53.45	52.24	10.10	65.46	64.49	6.97
Ni	4.58	13.06	15.42	4.76	17.09	26.15	3.46	12.52	22.69

3.2 Application of Synthesized MOFs

Batch adsorption studies were conducted on three types of dyes; Anionic (Congo Red), Cationic (Crystal violet) and pH indicator (Methyl Orange). The results indicate good adsorptive removal for anionic and cationic dye but less for pH indicator (see Fig. 4). All adsorbents showed removal behavior in the order Congo Red > Crystal violet > Methyl Orange. The reason for high adsorptive

removal of anionic dye could be because of development of positive charge on the surface of adsorbent leading to more interaction with anionic dyes [15]. On the other hand, adsorption of cationic dyes (methyl orange) on the positive surfaces may be hindered by cationic-cationic repulsion. Beside that the presence of unbounded COO^- groups may favor crystal violet adsorption on the surface due to electrostatic interaction [16]. The adsorptive removal of pH indicator dye was less because of its pH depending nature. Further, the basic aqueous solution of Methyl orange was used and for good cation removal, higher pH is required. This condition is caused due to deposition of OH^- ions on adsorbent surfaces [17].

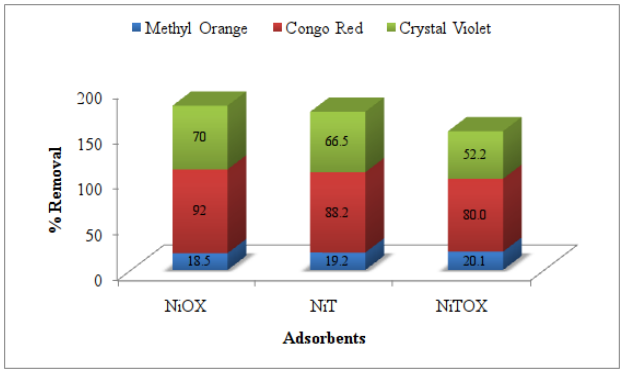

Fig. 4. Efficiency of synthesized MOFs as adsorbents for removal of dyes

3.2.1 Effect of Contact Time

Effect of contact time to study the adsorption was studied to establish equilibrium between adsorbent and adsorbate. For this purpose effect of contact time was studied at different initial concentrations and adsorbent doses (see Fig. 5). Most of the results indicated the regular increase in percent removal of Methyl orange upto 10min and after that there was decrease in percent removal due to desorption phenomenon. The initial high percent removal was due to presence of abundant binding sites [18]. There was irregular trend for the attainment of equilibrium but for the batch experiments the equilibrium time was between 15- 25min.

The results of effect of contact time for Congo Red also indicated rapid adsorption removal at early stage due to increase in available sites. After 15min to 20min equilibrium was achieved which further result in desorption phenomena.

Adsorption removal of crystal violet with relation to contact time presented the decreasing trend why may be result of earlier desorption due to cationic-cationic hindrance. The equilibrium attained for crystal violet removal was in range 10-15min.

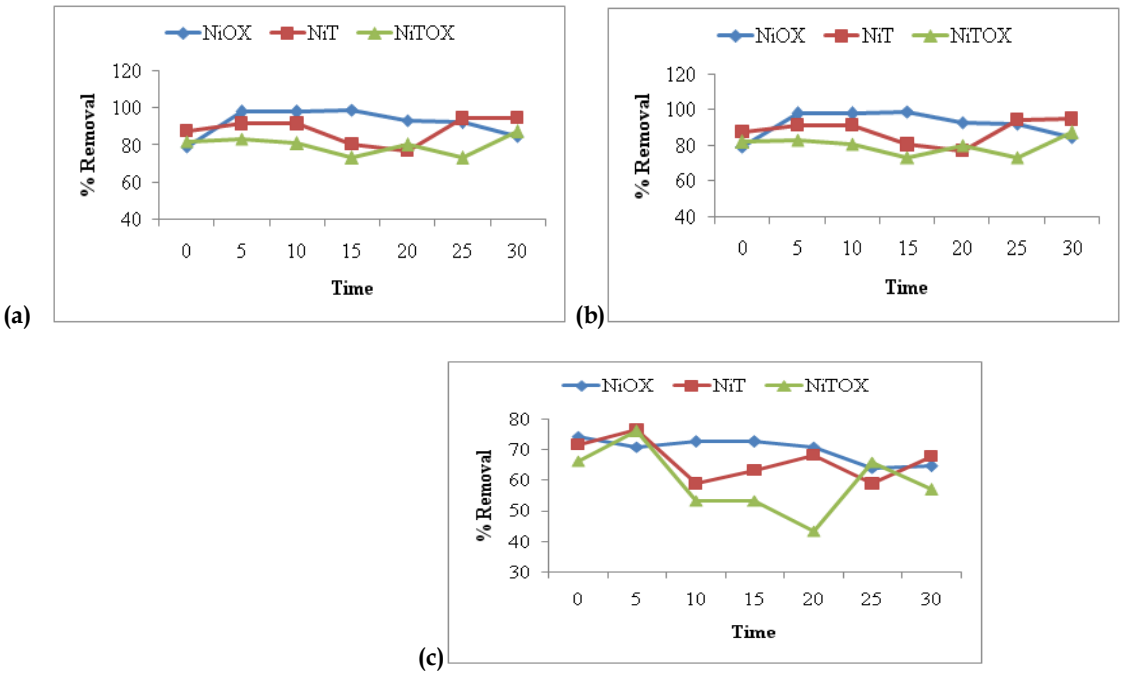

Fig. 5. Effect of contact time for removal of (a) Methyl Orange (b) Congo Red (c) Crystal Violet

3.2.2 Effect of Adsorbent dose

Effect of adsorbent dose at given induced concentration was studied to check the adsorption capacity of synthesized MOFs. Each batch experiment was done at 2mg, 5mgand 10mg of each adsorbent with induced concentration of 0.01mg/L, 0.03mg/L and 0.05mg/L of induced concentration of dyes.

The results presented in Fig. 6(a) indicated that as the mass of adsorbent increased, removal of Methyl Orange also increased. This change in removal was abrupt when concentration increased from 1mg to 5mg while this change was minor when dose was increased to 10mg. this increase in removal percentage could be due to increase in available sorption surface area and adsorption sites [19].

The results presented in Fig. 6(b) indicated overall good adsorption for Congo Red with no specific trend. The adsorbents NiT showed increasing trend with increase in dose due to availability of more adsorbent sites. The decreasing trend shown by other adsorbents could be due to inhibition of diffusion as a result of increasing viscosity caused by high adsorbent dose [20].

For Crystal violet, the adsorbents NiOX and NiT presented decreasing trend as the dose increases this could be due formation of agglomerates of adsorbent particles at higher dose [21].

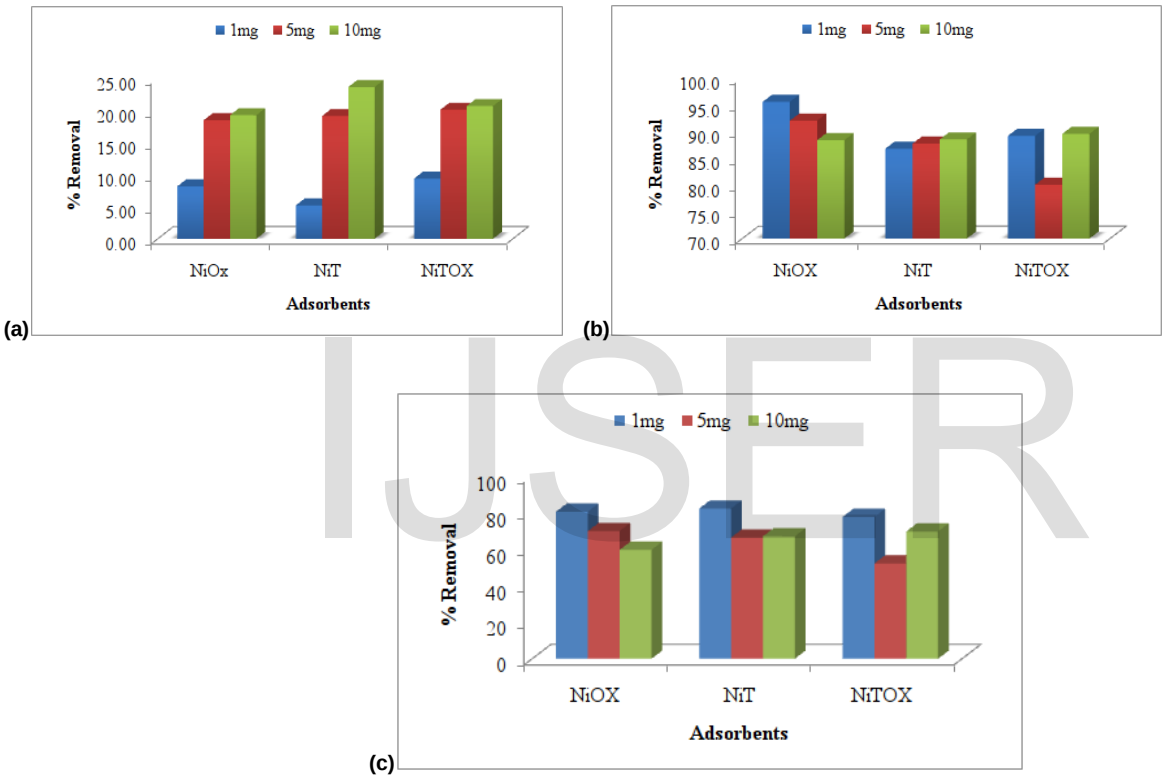

Fig. 6: Effect of adsorbent dose for removal of (a) Methyl Orange (b) Congo Red (c) Crystal Violet

3.2.3 Effect of Induced Concentration

Three different concentrations (0.01mg/L, 0.03mg/L and 0.05mg/L) of Methyl Orange were introduced on three different mass variations of adsorbents (1mg/Kg, 5mg/Kg, 10mg/Kg). The results shown in Fig. 7(a) indicated the variable trend with increasing the concentration at different doses. This variable trend could be attributed to specific available sites for adsorption and also could be result of provision of necessary driving forces to overcome the confrontation between solid-liquid phases [22].

Percent removal of Congo Red presented Fig. 7(b) indicated interesting increasing adsorption The increase in concentration could be result of increase in forces which decrease resistance to mass transfer between liquid and solid phases.

In case of crystal violet, the adsorbent NiOX showed decrease in percent removal with increasing the induced concentration indicating the limited sites for adsorption of guest molecules. The adsorbents NiT, NiTOX represented increase in adsorption at 0.05mg/L indicating decrease in resistance against concentration gradient [23].

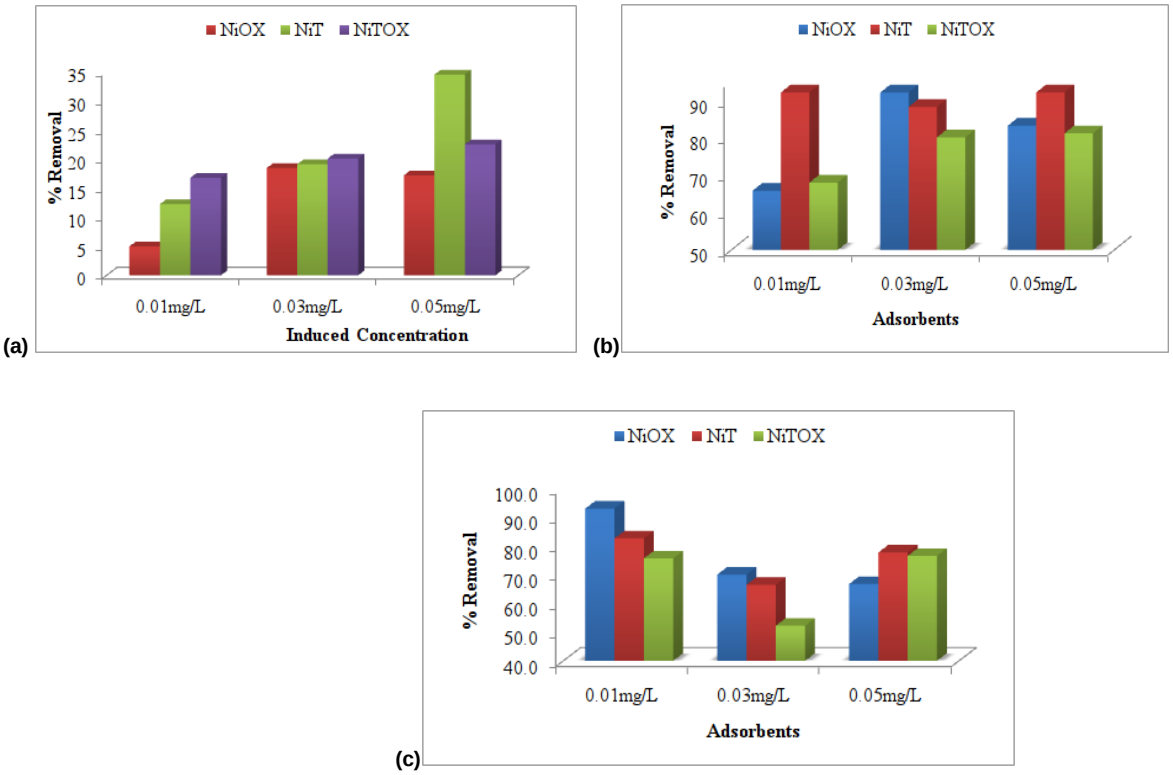

Fig. 7. Effect of Induced concentration for removal of (a) Methyl Orange (b) Congo Red (c) Crystal Violet

3.2.4 Effect of Temperature

Batch experiments were conducted at three different temperatures i.e. 25°C, 50°C and 70°C for 5mg dose and 0.03mg/L initial concentration. The results indicated the increase in adsorption upto 50°C which further decreased upto certain limit when temperature increased to 70°C. The increase in percent removal could be result of decrease in particle density which create more reactive sites and thus increase the penetration of guest molecules in micropores [24]. The decrease in adsorption at 70°C could be result of increase in kinetic energy which makes the reaction exothermic and thus dye desorbs early at elevated temperature [25].

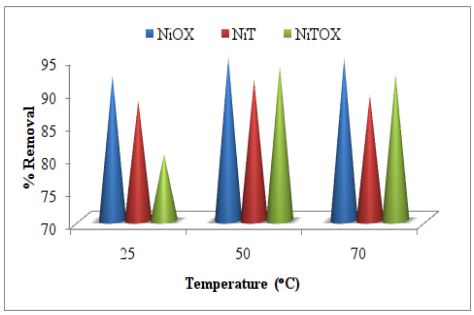

Fig. 8. Effect of Temperature for removal of dye

3.2.5 Adsorption Isotherm and Kinetics

Kinetic study of the adsorption gives an important insight to understand the mechanism of adsorption. The adsorption kinetics and isotherm models were applied on batch experiments for removal of azo dyes. Equilibrium Isotherms are used to quantify the adsorptive capacity of three adsorbents while kinetic data is used to predict the rate at which the adsorbates are removed from the solution. Isotherm studies were conducted using three models i.e. Freundlich, Langmuir and Temkin. The isotherm studies indicated that the adsorption of all pollutants followed the Freundlich and Temkin model. In order to investigate the sorption kinetics of pollutants, first order, pseudo first order, pseudo second order and intra-particle diffusion were applied to fit the experimental data. The results

indicated the pseudo second order the best fit model to explain the adsorption kinetics.

Table 2: Adsorption isotherms of dyes

Dyes	Adsorbent	Isotherm Models								
		Freundlich			Langmuir			Temkin		
		K_F	n	R^2	K_L	q_m	R^2	K_T	B_1	R^2
Methyl Orange	NiOX	- 8.199	-3.688	0.995	961.3	-18.9	0.967	-0.163	-0.047	0.999
	NiT	- 9.217	-4.313	0.992	1543	-33.61	0.988	-0.168	-0.048	0.999
	NiTOX	- 8.778	-4.041	0.979	869.5	-16.68	0.923	-0.166	-0.047	0.999
Congo Red	NiOX	-1.755	-0.069	0.851	38.59	-0.002	0.818	0.033	-0.001	0.869
	NiT	-1.924	-0.137	0.953	43.53	-0.014	0.818	0.026	-0.000	0.963
	NiTOX	-2.167	-0.244	0.976	51.56	-0.055	0.905	0.024	-0.000	0.984
Crystal Violet	NiOX	-2.6	-0.449	0.996	70.31	-0.2	0.986	-0.045	-0.018	0.998
	NiT	-2.199	-0.256	0.965	53.54	-0.058	0.883	-0.014	-0.012	0.980
	NiTOX	-3.233	-0.771	0.972	105.4	-0.575	0.896	-0.078	-0.025	0.991

Table 3: Kinetic models of dyes

Dyes	Adsorbent	Kinetic Models					
		Pseudo-2nd order			Intra-particle		
		K_2	q_e cal	R^2	A	K_{id}	R^2
Methyl Orange	NiOX	188.9	- 279.9	0.987	-0.003	1.368	0.462
	NiT	180.4	- 153.8	0.959	0.003	1.224	0.157
	NiTOX	147.5	63.60	0.951	0.005	1.236	0.374
Congo Red	NiOX	9E-05	-1.561	0.992	9E-05	1.961	0.000
	NiT	0.000	-1.584	0.975	0.000	1.938	0.013
	NiTOX	-0.000	-1.616	0.981	-0.000	1.906	0.008
Crystal Violet	NiOX	51.83	-38.70	0.994	-0.002	1.874	0.720
	NiT	48.86	-57.84	0.981	-0.003	1.955	0.732
	NiTOX	57.91	47.37	0.934	-0.001	1.763	0.032

4 CONCLUSION

The present study concluded the successful synthesis of MOFs based on oxalic acid and trimesic linkers with good metal incorporation using ambient conditions.

The effort to synthesize new mixed ligand metal organic framework was also successfully achieved which provided new structures to be used for further application.

XRD and SEM analysis also verified the synthesis of MOFs due to formation of crystal structures.

The sequence of average removal of dyes at optimum operating conditions followed the order Congo Red > Crysal Violet > Methyl Orange.

Anionic pollutants were best candidate being adsorbed i.e. Congo Red due to cationic and hydrophilic nature of adsorbents.

The best fit isotherm was Freundlich following pseudo second order kinetics.

The synthesized MOFs were also found to be appropriate for removal of pollutants from industrial waste.

The present recommended the use of controlled conditions for better nucleation and growth of crystals.

The synthesized product can also be used for future applications of catalytic degradation of pollutants.

REFERENCES

[1] WHO, "*Health risks of persistent organic pollutants from long-range transboundary air pollution*". Copenhagen, Denmark: World Health Organization, 2003.

[2] J. M. Yang, Q. Liu, and W. Y. Sun, "Shape and size control and gas adsorption of Ni (II)-doped MOF-5 nano/microcrystals". *Microporous and Mesoporous Materials*, vol. *190*, pp. 26-31. 2014.

[3] A. C. McKinlay, R. E. Morris, P. Horcajada, G. Ferey, R. Gref, and P. Couvreur, "BioMOFs: metal-organic frameworks for biological

and medical applications". *Angewandte Chemie International Edition,* vol. 49 no.36, pp. 6260-6266, 2010.

[4] M. Eddaoudi, J. Kim, N. Rosi, D. Vodak, J. Wachter, M. O'Keeffe, and O. M. Yaghi, " Systematic design of pore size and functionality in isoreticular MOFs and their application in methane storage". *Science,* vol. 295, no. 5554, pp. 469-472, 2002.

[5] X. Li, L. Zheng, L. Huang, O. Zheng, Z. Lin, L. Guo, B. Qiu, and G. Chen, "Adsorption removal of crystal violet from aqueous solution using a metal-organic frameworks material, copper coordination polymer with dithiooxamide". *Journal of Applied Polymer Science*, vol. 129, no. 5, pp. 2857-2864, 2013.

[6] E. Haque, V. Lo, A. I. Minett, A. T. Harris, and T. L. Church, "Dichotomous adsorption behaviour of dyes on an amino-functionalised metal–organic framework, amino-MIL-101 (Al)". *Journal of Materials Chemistry A*, vol. 2, no. 1, pp. 193-203, 2014.

[7] Z. Carmen, and S. Daniela, "*Textile Organic Dyes " Characteristics, Polluting Effects and Separation/Elimination Procedures from Industrial Effluents": A Critical Overview,* 2012.

[8] H. Wang, S. J. Liu, D. Tian, J. M. Jia, and T. L. Hu, "Temperature-Dependent Structures of Lanthanide Metal-Organic Frameworks Based on Furan-2, 5-Dicarboxylate and Oxalate". *Crystal Growth and Design, vol.* 12 no. 6, pp. 3263-3270, 2012.

[9] R. L. Frost, J. Yang, and Z. Ding, "Raman and FTIR spectroscopy of natural oxalates: Implications for the evidence of life on Mars". *Chinese Science Bulletin,* vol. 48, no.17, pp. 1844-1852, 2003.

[10] A. Rios-Ramos, C. Rivera-Maldonado, G. I. Garcia-Acosta, C. M. Lozano-Paulino, P. M. Fierro-Mercado, L. Fuentes-Cobas, and R. M. Roque-Malherbe, "Synthesis, structure, adsorption space and magnetic properties of Ni-oxalate porous molecular magnet". *Journal of Materials Science and Engineering A: Structural Materials: Properties, Microstructure and Processing, vol.* 2, no. 3, pp. 284-301, 2012.

[11] Y. Ge, H. Adler, A. Theertham, L. L. Kesmodel, and S. L. Tait, "Adsorption and Bonding of First Layer and Bilayer Terephthalic Acid on the Cu (100) Surface by High-Resolution Electron Energy Loss Spectroscopy".*Langmuir*, vol. 26, no. 21, pp. 16325-16329, 2010.

[12] H. Zhang, R. Xiao, M. Song, D. Shen, and J. Liu, "Hydrogen production from bio-oil by chemical looping reforming". *Journal of Thermal Analysis and Calorimetry*, vol. 115, no. 2, pp. 1921-1927, 2014.

[13] C. Chmelik, J. Karger, M. Wiebcke, J. Caro, and J. M. Baten, "Adsorption and diffusion of alkanes in CuBTC crystals investigated using infra-red microscopy and molecular simulations". *Microporous and Mesoporous Materials*, vol. 117, no. 1, pp. 22-32, 2009.

[14] N. T. Binh, D. M. Tien, L. T. K. Giang, H. T. Khuyen, N. T. Huong, and T. T. Huong, "Study on preparation and characterization of MOF based lanthanide doped luminescent coordination polymers". *Materials Chemistry and Physics*, vol. 143, no. 3, pp. 946-951, 2014.

[15] K. G. Bhattacharyya, & A. Sharma, "Kinetics and thermodynamics of Methylene Blue adsorption on Neem (*Azadirachta indica*) leaf powder". *Dyes and Pigments,* vol. 65, no. 1, pp. 51-59, 2005.

[16] V. P. Mahida, and M. P. Patel, "Removal of some most hazardous cationic dyes using novel poly (NIPAAm/AA/N-allyl isatin) nanohydrogel". *Arabian Journal of Chemistry,* 2014.

[17] M. J. Iqbal, and M. N. Ashiq, "Thermodynamics and kinetics of adsorption of dyes from aqueous media onto alumina". *Journal of the Chemical Society of Pakistan*, vol. *32*, pp. 419-428, 2010.

[18] B. H. Hameed, and A. A. Ahmad, "Batch adsorption of methylene blue from aqueous solution by garlic peel, an agricultural waste biomass". *Journal of hazardous materials, vol.* 164, no.2, pp. 870-875, 2009.

[19] H. Chen, J. Zhao, J. Wu, and G. Dai, "Isotherm, thermodynamic, kinetics and adsorption mechanism studies of methyl orange by surfactant modified silkworm exuviae". *Journal of hazardous materials*, vol. 192, no. 1, pp. 246-254, 2011.

[20] Y. Yao, H. Bing, X. Feifei, and C. Xiaofeng, "Equilibrium and kinetic studies of methyl orange adsorption on multiwalled carbon nanotubes". *Chemical Engineering Journal, vol.* 170, no. 1, pp. 82-89, 2011.

[21] B. V. Rao, K. Ramanjaneyulu, T. B. Rao, and T. Rambabu, "Synthesis and bioactivity evaluation of cinnamic acid esters from oxalis pes-caprace". *Journal of Chemical and Pharmaceutical Research, vol.* 3, no. 2, pp. 589-594, 2011.

[22] N. Tabassum, U. Rafique, K. S. Balkhair, and M. A. Ashraf, "Chemodynamics of methyl parathion and ethyl parathion: adsorption models for sustainable agriculture". *BioMed research international*, 2014.

[23] R. Dongre, M. Thakur, D. Ghugal, and J. Meshram, "Bromine pretreated chitosan for adsorption of lead (II) from water". *Bulletin of Materials Science, vol.* 35, no. 5, pp. 875-884, 2012.

[24] M. Al-Ghouti, M. A. M. Khraisheh, M. N. M. Ahmad and S. Allen, "Thermodynamic behaviour and the effect of temperature on the removal of dyes from aqueous solution using modified diatomite: a kinetic study". *Journal of Colloid and Interface Science, vol.* 287, no. 1, pp. 6-13, 2005.

[25] Y. S. Al-Degs, M. I. El-Barghouthi, A. H. El-Sheikh, and G. M. Walker, "Effect of solution pH, ionic strength, and temperature on adsorption behavior of reactive dyes on activated carbon". *Dyes and Pigments, vol.* 77, no. 1, pp. 16-23, 2008.